Generator Protection Validation Testing Using a Real-Time Digital Simulator: Stator Winding Protection

Ali B. Dehkordi, *RTDS Technologies Inc.*
Ritwik Chowdhury, Normann Fischer, and Dale Finney, *Schweitzer Engineering Laboratories, Inc.*

***Abstract*—Correct operation of generator protection is critical to avoid forced outages and to minimize damage during internal faults and other abnormal events. Testing security for external faults and system disturbances has been carried out in the past using real-time systems or transient simulation software. Scaled physical models have been employed to simulate internal faults. However, these machines are restricted in the types of faults that can be applied and the variety of systems that can be modeled.**

This paper describes a new synchronous generator model that has been developed in a real-time digital simulator. The model can be configured with a wide range of electrical and mechanical parameters and can simulate various types of faults both on the rotor and on the stator.

The paper also describes how the new model was used to validate a new multifunction generator protection relay. The relay incorporates several novel protection elements, so comprehensive validation of these elements was very important. A wide range of faults were applied, including external faults, power swings, stator winding faults, field short-circuits, and faults during static starting.

This paper focuses on stator winding protection for ground faults, phase faults, turn-to-turn faults, and series faults. The performance of the protection was measured for these events. Application guidance for stator ground, split-phase, and negative-sequence directional protection for generators is provided.

I. Introduction

Microprocessor generator relays integrate numerous protection elements into a single device. Each element is designed to detect a particular type of internal fault or abnormal condition and to initiate a specific tripping sequence. Commissioning testing is carried out for a particular application to confirm that each element has the correct settings and that the relay is working correctly. In contrast, validation testing confirms that the hardware, analog and digital signal processing, and protection elements are fit-for-purpose and verifies the correct response to all events, including the following:

- Internal faults
  - Phase-to-phase faults (or simply phase faults)
  - Phase-to-ground fault (or simply ground faults)
  - Turn-to-turn faults (or simply turn faults)
  - Series faults
- External faults
- Motoring
- Overexcitation
- Loss of excitation or underexcitation
- Inadvertent energization
- Stuck breaker (one or more poles)
- Faults during static starting
- Stressed power system
  - Stable or unstable power swings
  - Generation or load rejection
  - Islanding
- Instrument transformer misbehavior

In the past, scaled physical models have been used for validation testing [1]. These models are useful but are limited in the size and type of generator and the characteristics of the connected power systems that can be simulated.

Considerable research has been carried out to develop methods for simulation of generator internal faults [2]–[7] dating back to the early days of mainframe computers. Most of these methods replace the sinusoidal spatial distribution of the magnetomotive force (MMF) with the concept of a winding function. Some methods use the operational parameters of the machine (X_d, X_q, X'_d, etc.), while others require more detailed information about the winding (pitch factor, distribution factor, etc.). Many of the previous efforts were not designed for integration into an electromagnetic-transient-type (EMT-type) power system simulation program.

Recently, a synchronous generator model that is capable of modeling internal faults in the presence of parallel windings has been developed for a real-time digital simulator. This development allows for tens of thousands of cases to be tested with hardware in the loop. The simulation parameters can be varied quickly to cover a wide range of system configurations.

The new model was used to validate all of the protection elements provided by the new generator relay, including loss of field, motoring, and current unbalance. Complex scenarios, such as an internal fault during a power swing or an overexcitation during a load commutated inverter (LCI) start, were also tested. This paper includes only the results of the internal faults on the stator winding; the testing of the balance of protection elements will be covered in a future paper.

II. Description of the Faulted Synchronous Generator Model

This section briefly describes the analysis and modeling method of the faulted synchronous machine model developed in this paper. Because the goal is the incorporation of the model into an electromagnetic transient program [8], the coupled

electric circuit approach is used for the modeling of the synchronous machine. The method of calculating the inductances of faulted windings is briefly explained. The assumptions used for this analysis and the capabilities of the model are discussed in the following subsections.

A. Theoretical Background of the Model

As explained in the introduction, the faulted synchronous machine model was developed for the environment of the real-time digital simulator. The real-time simulator is a combination of computer hardware and software designed specifically for the solution of power system EMT in real time. Each unit of the simulator consists of processors (or cores) dedicated to the solution of the power system networks, power system devices, and control components [9]. Each simulation time-step is divided into computation intervals and communication intervals. As with other EMT programs, such as EMTP and EMTDC, Dommel's algorithm [8] is used for discretization of the electric system's differential equation. In this method, passive resistor, inductor, and capacitor (RLC) elements of the circuit, as well as more sophisticated components (such as machines, transformers, and power electronics), are represented by companion circuits in the form of current sources and conductances [8]. Subsequently, the nodal solution is used for the calculation of node voltages.

1) Embedded Solution for the Machine Model

A more precise method of developing the companion circuit of an electric machine model is called the *embedded* solution [10] [11] in this paper. Equation (1) shows the resulting discrete format of the machine phase domain equations obtained using trapezoidal integration. In (1), [L] is the inductance matrix of the machine and [R] is the diagonal matrix representing the winding resistances, where v(t) and i(t) are the voltages and currents of the windings at every time step. Matrix $[G_{EQ}(t)]$ represents the equivalent admittance matrix of the machine after discretization. This matrix must be processed by the main network solution of the EMT program in every time step. The vector $\underline{Ih}$ represents the history terms in the discretization process, which need to be injected to corresponding nodes as current sources.

$$\underline{v}(t)=\frac{d}{dt}\underline{\lambda}(t)+[R]\underline{i}(t)=\frac{d}{dt}\left\{[L(t)]\underline{i}(t)\right\}+[R]\underline{i}(t)$$

after discretizing using the trapezoidal integration:

$$\underline{i}(t)=\left[G_{EQ}(t)\right]\underline{v}(t)+\underline{Ih}$$

where: (1)

$$\left[G_{EQ}(t)\right]=\left[R_{EQ}(t)\right]^{-1}=\left\{\frac{2}{\Delta t}[L(t)]+[R]\right\}^{-1}$$

$$\underline{Ih}=\left[G_{EQ}(t)\right]\left\{\underline{v}(t-\Delta t)+\left[R'_{EQ}(t-\Delta t)\right]\underline{i}(t-\Delta t)\right\}$$

$$\left[R'_{EQ}(t-\Delta t)\right]=\frac{2}{\Delta t}[L(t-\Delta t)]-[R]$$

Such an elaborate method of implementation requires substantial computation resources [10] [11]; however, as shown in upcoming sections, this method provides important advantages for the model.

2) Calculation of Phase Domain Inductances

Another important theoretical aspect of the model is the calculation of the machine inductance matrix and the assumptions that are made. The inductance matrix of the machine plays an important role in defining the dynamics of the machine, including its behavior during internal faults. Because the electric coupled circuit approach, shown in (1), was chosen as the method of simulation, the main task remaining was calculating the inductances of the machine (including faulted windings). There are various methods available for evaluating these inductances. These include actual measurement of inductances [12] [13], finite-element-method-based (FEM-based) methods [14], and the modified winding function approach (MWFA) [15] [16]. In comparison to the MWFA, the FEM provides results that are more precise; however, it requires significantly more information about the design of the machine, which is not readily available to most users of EMT programs.

In addition to so-called standard d-q data (i.e., steady-state, transient and sub-transient reactances, and time constants), the MWFA also requires certain information about the design of the machine, such as the distribution of the windings. This presents hurdles in the widespread use of such models. The authors in [17] and [18] proposed a method in which the need for information about the distribution of the windings is eliminated. In this approach, it is assumed not only that the healthy windings create a perfect, sinusoidally distributed MMF, but also that the MMF due to the subwindings is sinusoidal. In this paper, each stator winding is divided into two or more partitions called subwindings. The idea is that each subwinding produces a sinusoidal MMF and, based on that, an effective turns-ratio and an effective angle is calculated for each subwinding. This approach, in essence, is equivalent to the winding function approach that neglects the space harmonics. This assumption allows for the analytical calculation of subwinding inductances.

Based on the above description, the method of [17] and [18] with certain enhancements is used in this paper to calculate the inductances of subwindings.

B. Model Assumptions

1) Representation of Slot and Space Harmonics

As mentioned earlier, the proposed model is intended for users who might not have access to design data, such as distribution of the windings. Naturally, this model is not capable of representing the effects of slot harmonics and the phase-belt harmonics (the 3rd, 5th, and 7th harmonics) due to the nonsinusoidal distribution of the windings and permeance.

2) Calculation of Subwindings Leakage Inductance

Turn-to-turn faults are influenced by the winding distribution and, more importantly, the leakage inductances. Once a winding is divided into two or three sections, which is the case in this model, the leakage and magnetizing portions of inductances are also divided among the subwindings. One of the challenges of this method is dividing the leakage portion of the original winding inductance among the subwindings. The stator leakage inductance is comprised of several components, such as slot leakage inductance, zigzag leakage inductance,

phase-belt leakage inductance, and so on. Accurate division of the leakage inductance among the subwindings requires detailed knowledge of the winding distribution and the geometry of the machine. In the proposed model, the leakage inductances are simply divided based on the accumulated number of turns in each series subwinding.

3) Representation of Damper Grid

Another factor in the modeling of turn faults in synchronous machines is the representation of the rotor damper grid. In the proposed faulted synchronous machine model, the rotor damper grid is modeled as one or two windings along the d- and q-axes, which is the conventional method of modeling damper grids in system studies [19]. It has been shown that this representation, in rare occasions, may cause significant errors in modeling turn faults for multiple pole synchronous machines [13]. Alternatively, one d-axis damper winding and one (or two) q-axis damper windings must be considered for each pole of a synchronous machine for accurate simulation of bolted turn faults [6]. It should be noted that such comprehensive representation of the damper grid requires detailed knowledge of machine design as well as a significant increase in the computational capacity of the simulator. On a positive note, this error is less significant for machines with only two poles or machines with a much higher number of poles with practical distribution for the windings.

4) Treatment of Parallel Windings

Most multipole synchronous generators use parallel stator windings in their designs. The number of parallel windings can be as large as the number of pole pairs. One of the advantages of the model presented here is the capability of modeling machines with parallel windings.

To connect two magnetically coupled windings in parallel, the two windings need to be identical. Otherwise, a large flow of circulating current results. Based on this design criterion, the parallel windings for each stator phase of the machine are assumed identical (they have an equal electrical angle and the same number of turns). In practical designs, different parallel windings face different pole-pairs of the generator. This causes parallel windings to have an identical electrical angle, but a different mechanical angle. However, in the current model, it is assumed that the two parallel windings in the model face the same poles.

C. Capabilities of the Model and Simulation Results

Based on the above analysis and assumptions, a real-time faulted synchronous machine model capable of modeling internal faults was developed. The model provides two parallel paths for the stator windings. Experimental validation of the model is not the focus of this paper; instead, the paper uses the flexibility of this model to validate several protection elements in a new generator relay and provide associated application guidance. (Note that the above techniques and assumptions have been previously validated [10]–[18].)

The model has the following capabilities and features. In the presence of parallel windings, the model allows users to apply turn-to-turn faults in one branch as well as in the field winding, faults between phases, and faults between different parallel branches of the same phase. A feature of the embedded phase domain approach, introduced in the previous section, is that it provides superior numerical stability and adds to the flexibility of the model. This allows users to access faulted junctions of the windings as independent nodes in the circuit. This in turn provides the capability of modeling series faults in which the occurrence of fault causes an open circuit or an increase in the impedance of the junction through arcing.

The icon for the model in this configuration is shown in Fig. 1. Each stator winding has two parallel paths (branches), and each branch is divided into two subwindings, resulting in 12 total subwindings. All 24 nodes of these subwindings are available to the user to be connected to other power system components, such as grid components, fault impedances, and arc models. A similar arrangement is made for the field winding. This provides great flexibility in testing generator protection schemes.

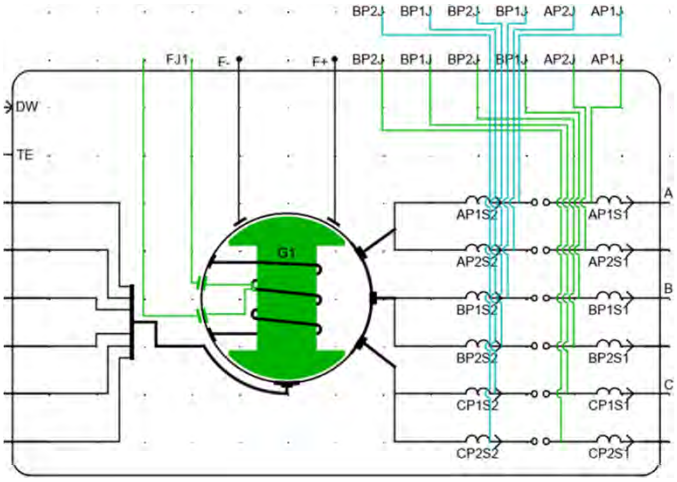

Fig. 1. Generator component suitable for ground, phase, and series faults

D. Modeling of Inherent Unbalance in the Original Windings

It is often desirable to simulate synchronous machines with unbalanced windings. This unbalance can be caused by one of the windings having a different number of turns than the windings in other phases or parallel paths, which in turn deviates the effective number of turns and effective angle for that winding from ideal values. The model introduced here allows users to simulate such conditions by deviating the effective number of turns and effective angle of a certain winding by a few percentages and a few degrees, respectively. The simulations associated with such unbalance are provided in Section IV.E.3.

III. Generator Relay and Protection Elements

The generator protection relay validated in this paper has 6 voltage inputs and 18 current inputs that can be configured for a wide range of applications. It independently tracks generator and system frequency over a range from 5 to 120 Hz. A simplified description of the protection elements (for the scope of this paper) is provided in this section; more details can be found in [20]. A summary of the relay settings used for this paper is provided in the appendix.

A. Fundamental Neutral Overvoltage (64G1)

The 64G1 element is the primary means of stator ground fault protection and is usually set to cover 90% to 95% of the stator winding. This translates to a low pickup setting. Consequently, the element can assert for a ground fault on the voltage transformer (VT) secondary or the system fault coupling through the generator step-up (GSU) interwinding capacitance [21]. Because of this, the element is time-delayed to coordinate with VT fuses and system protection.

Most stator ground faults begin as intermittent faults [22]. Therefore, time coordination reduces dependability of the 64G1 element [21]. The validation relay provides an acceleration path with an integrating timer to improve the dependability of this element, as shown in Fig. 2.

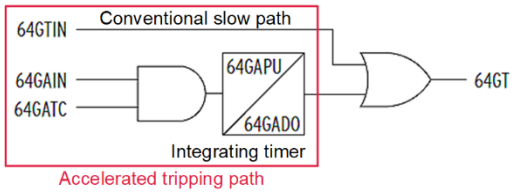

Fig. 2. Stator ground protection with accelerated tripping

B. Third-Harmonic Schemes (64G2/64G3)

Third-harmonic schemes (either or both the 64G2 and 64G3 elements) can be applied to provide 100% coverage for stator ground faults when combined with 64G1. The difference between the 64G2 and 64G3 elements is that 64G2 requires a third-harmonic survey and therefore is more difficult to set. However, 64G2 can protect a greater percentage of the winding when the third-harmonic produced by the generator is large, unlike 64G3, which protects a fixed percentage (e.g., 15%) of the winding [23]. Additionally, 64G2 can trip for intermittent faults quicker than 64G3, which is shown in Section V.A.2.

C. Generator Differential (87G)

The 87G element detects phase faults in a high-impedance grounded generator. The validation relay has two zones and the adaptive characteristic shown in Fig. 3 [24].

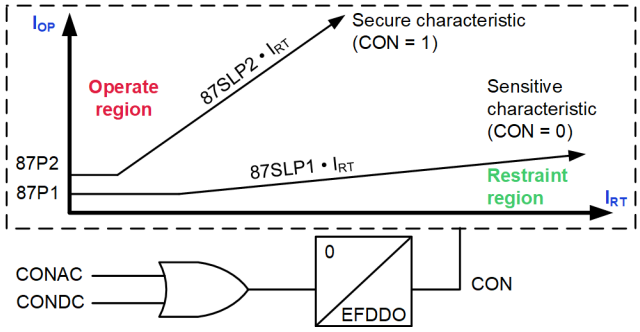

Fig. 3. Differential element with adaptive sensitive and secure characteristic

The relay normally uses a sensitive characteristic with a pickup (87P1) and a slope (87SLP1). The relay adapts to using a secure characteristic to prevent a possible misoperation due to current transformer (CT) saturation when the external fault detector (CON) asserts. CON may assert if either CONAC or CONDC assert. CONAC is associated with a sudden increase in restraint current (IRT) without an associated increase in the operate current (IOP) current. CONDC is associated with the presence of large dc in the currents comprising the 87G element.

D. Negative-Sequence Directional (67Q)

The 67Q element is not commonly applied for generator protection. It is, however, a relatively simple way to detect certain unbalanced faults (such as turn faults) that might not be otherwise detected by the differential or ground fault protection elements. This element operates on negative-sequence current (I_2) and is polarized by negative-sequence voltage (V_2), both measured at the generator terminals. The 67Q element operates if the conditions of (2) are true, which depends on the magnitude of I_2 during the fault (and is further discussed in Section V.C.2).

$$67Q = 50Q \text{ AND } F32Q \tag{2}$$

where:

67Q indicates the element pickup.

50Q is the pickup of the overcurrent element.

F32Q is the forward declaration (internal fault indication) from the negative-sequence directional element.

E. Split-Phase Overcurrent (60P/60N)

These elements are intended for turn fault detection but can also respond to phase-to-phase and branch-to-branch faults. The 60P element responds to individual phase currents. The 60P element can be connected to either a window-type CT or two external CTs connected differentially [25]. The 60N element connects to an interneutral CT if available. Since this element does not see load current, a low-ratio CT is used.

The 60P element provides high-set (conventional) and low-set (adaptive) stages, as shown in Fig. 4 and Fig. 5, respectively (60N is similar). Generators typically have a steady-state circulating current between branches of the same phase that can slowly change under normal operation. The steady-state current can be significant, especially on generators that have undergone temporary repairs [26]. This steady-state current limits the sensitivity of the conventional, high-set scheme of Fig. 4.

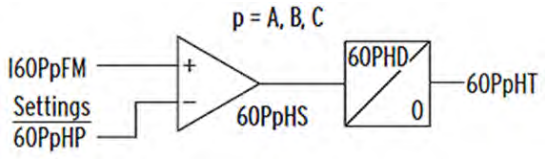

Fig. 4. High-set (conventional) split-phase element

The low-set stage of Fig. 5 is adaptive, allowing it to compensate for the variation in steady-state circulating current to obtain a secure and dependable operating current (I60PpOP).

The tracking algorithm uses a low-pass filter that resets its output when abrupt changes in the circulating current are expected; for example, when the generator is synchronized to the power system. In addition, the time delay can be increased dynamically to add security, such as when an external fault is detected by the 87G element.

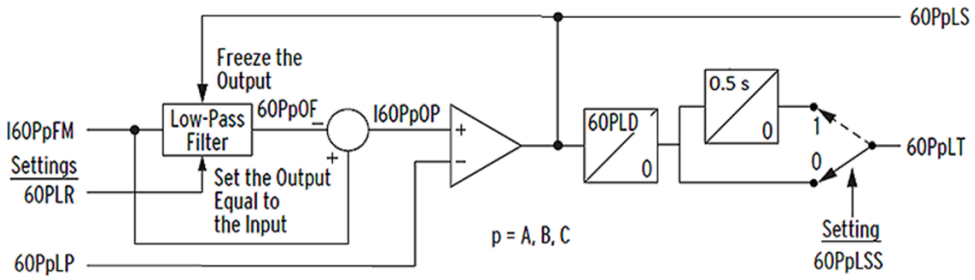

Fig. 5. Low-set (adaptive) split-phase element

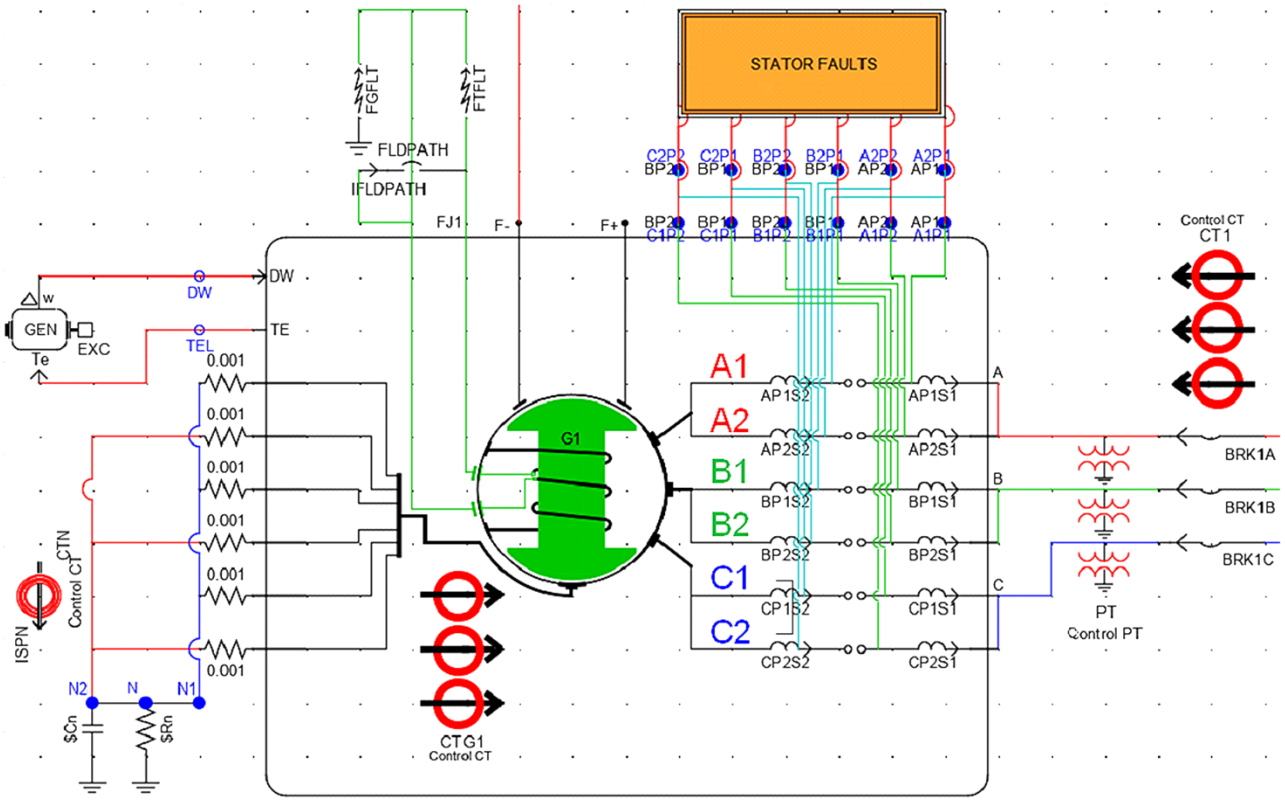

Fig. 6. Generator model interfaced with the power system

IV. Test Setup

A. Generator Model Interface and Parameters

The synchronous generator model described in Section II has two branches per phase, as shown in Fig. 6. Branch 1 of each of the three phases (A1, B1, and C1) was connected at the neutral to form one neutral (N1). Branch 2 of each of the three phases (A2, B2, and C2) was connected at the neutral to form the second neutral (N2). A low-ratio interneutral CT (CTN) with a turns ratio of 100 was applied to measure the circulating current between N1 and N2. The two neutrals were then connected to a common neutral.

The relevant generator and system parameters are provided in Table I, with all the impedances referenced to the generator impedance base (Z_{BASE}). The generator neutral was grounded via a high-impedance grounding resistor that was sized to match the total capacitance (C_G + C_X). The generator stator capacitance (C_G) was split equally using the pi-section model between the terminal and neutral [23].

TABLE I
GENERATOR AND SYSTEM PARAMETERS

Parameter	Value
Rated MVA and frequency	555 MVA, 60 Hz
Nominal voltages (V_{NOM} and V_{NOMLG})	24 kV, 13.86 kV
Nominal current (I_{NOM}) and impedance (Z_{BASE})	13.35 kA, 1.038 Ω
Impedances for d-axis (X_d, X_d', and X_d'')	1.81, 0.30, and 0.23 pu
Impedances for q-axis (X_q, X_q', and X_q'')	1.76, 0.65, and 0.25 pu
Stator leakage reactance (X_l)	0.10 pu
Generator zero-sequence reactance (X_0)	0.15 pu
Stator resistance (R_S)	0.003 pu
Neutral grounding resistance (R_N)	1,000 Ω primary
Generator stator capacitance (C_G)	0.684 µF
Additional terminal-side capacitance (C_X)	0.200 µF
Transformer impedance (X_T)	0.08 pu
System impedance (X_{SYS})	0.035 pu

The stator internal fault model of Fig. 6 is detailed further in Fig. 7 and was used to apply ground, phase, and series faults.

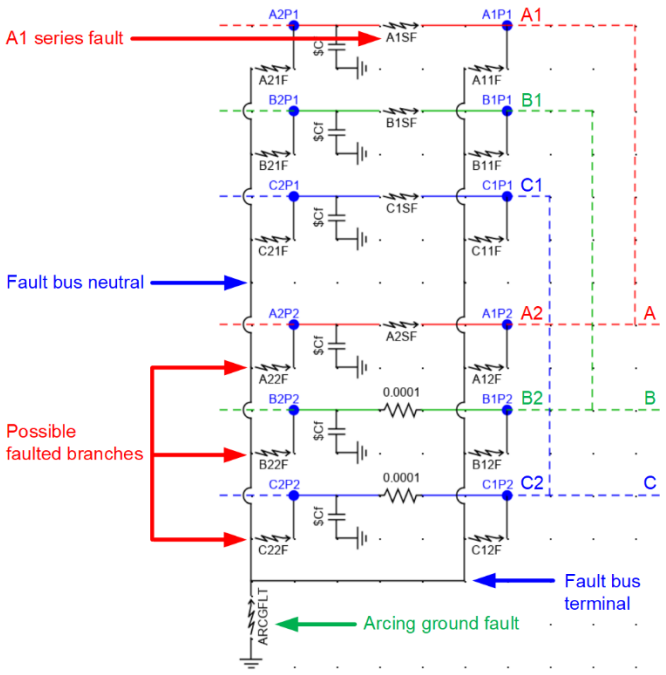

Fig. 7. Stator internal fault model used for ground, phase, and series faults

B. Generator Third-Harmonic Circuit

As noted in Section II.B, slot and space harmonics are not represented by the synchronous generator model. Generator relays often use third-harmonic schemes to provide neutral-side ground fault protection [23]. To test these schemes, a third-harmonic circuit that mirrored the fundamental circuit was implemented. The generated third-harmonic voltage (VG3) is a function of loading. This voltage in turn produces third-harmonic voltage at the terminals (VT3) and at the neutral of the machine (VN3). The voltage outputs of the fundamental and the third-harmonic circuits were then summated before being injected into the relay.

C. Generator Model to Relay Interface

The generator of Fig. 6 was protected by the generator relay under test using comprehensive protection, as shown in Fig. 8. The relay terminals, the instrument transformer ratios, and the descriptions are shown in Table II.

TABLE II
CURRENT AND VOLTAGE TERMINALS

Terminal	Rating	Application	Usage
VpZ	24,000:120 V	Generator terminal voltages from wye-grounded VTs	21, 24, 32, 40, 64G2, 64G3, 67Q, 78, and 81
IpW	20,000:5 A	Generator phase currents (neutral side)	21, 32, 40, 46, 78, and 87G
IpX	10,000:5 A	Split-phase current	60P
IY1	200:5 A	GSU neutral current	REF
IY2	500:5 A	Generator interneutral current	60N
IpS	20,000:5 A	Generator terminal currents	67Q, 87G, BF, BFO, and INAD
IpT	2,000:5 A	GSU high-voltage currents	87T
IpU	20,000:5 A	Generator low-voltage breaker currents	87T
VV1 (VAV)	24,000:120 V	System phase-to-phase voltage	25 and 25A
VV2 (VBV)	24,000:240 V	Generator neutral voltage	64G1, 64G2, and 64G3
VV3 (VCV)	24,000:120 V	Iso-phase bus $3V_0$ voltage from broken-delta VTs	64IPB

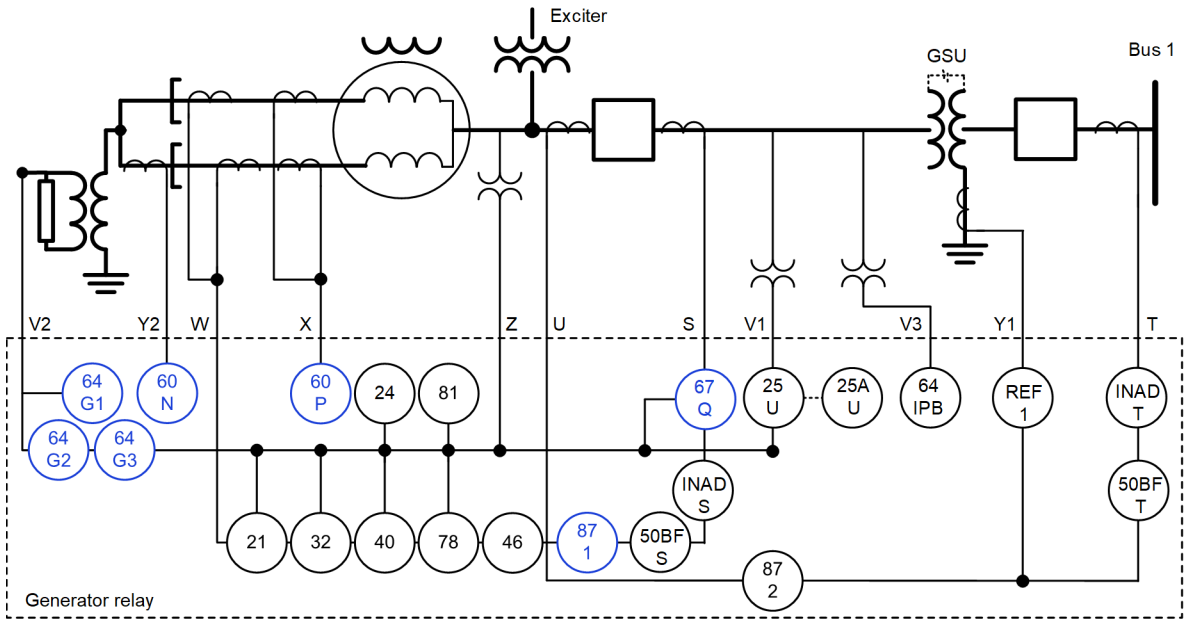

Fig. 8. Protection elements applied to protect generator

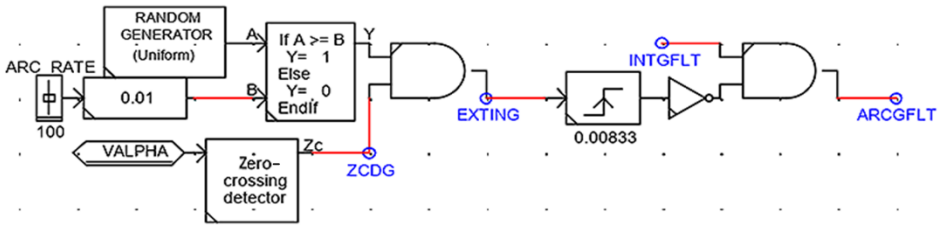

Fig. 9. Logic used to apply intermittent stator ground faults

D. Instrument Transformer Considerations

The CTs were modeled according to the requirements presented in [24]. The CTs providing phase currents to Terminals T, W, and X in Table II had a high burden, whereas those connecting to Terminals S and U had a low burden. This mismatch allowed verification of protection element security.

A V_2 supervision of 5% of V_{NOMLG} ($3V_2$ of about 10 V secondary) was added to the 64G acceleration scheme of Fig. 2 to achieve the following behavior.

- For a ground fault on the VT secondary that might cause the sensitively set 64G1 element to pick up, V_2 at the generator terminals is expected to be greater than 5%.
- For a stator ground fault, V_2 at the generator terminals is expected to be less than 5%, allowing the 64G elements to provide accelerated tripping.

E. Fault Model and Types

The dependability for the following stator winding internal faults was evaluated. The relay settings are provided in the appendix.

1) Intermittent Stator Ground Faults

Ground faults are the most common types of internal faults in a generator, and ground faults on a high-impedance grounded generator typically begin as intermittent faults [22].

To evaluate the dependability of the relay for intermittent ground faults, the logic of Fig. 9 was used. The response of the logic is shown in Fig. 10 for an arcing rate of 50% and explained as follows:

- At any given zero-crossing detected (ZCDG) of the alpha voltage, the ground fault can extinguish (EXTING). The alpha voltage (from Clarke's transformation) was used since it is not impacted by the stator ground fault and can be made to follow the voltage profile of the faulted phase.
- The arc rate was varied from 0% to 100% to simulate no-fault and sustained fault scenarios, respectively; values within the range correspond to an intermittent fault. A lower arc rate may correspond to faults that are at early stages of inception from insulation failure.
- The INTGFLT assertion corresponds to the duration that the internal ground fault is applied, and the ARCGFLT (arcing ground fault) drops out for half a cycle whenever the fault extinguishes. The randomized nature of an arcing fault is shown in Fig. 10.

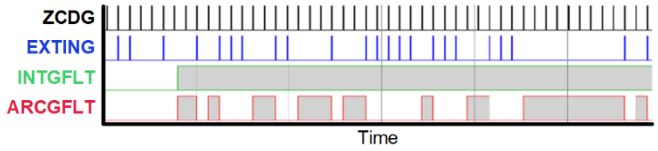

Fig. 10. Randomized nature of arcing for an intermittent fault

The performance of the ground fault protection elements for intermittent faults was evaluated at different loading levels and arcing rates; the results are shared in Section V.A.

2) Stator Winding Phase Faults

Phase faults are less common than other faults and abnormal conditions experienced by a generator, but they are very damaging. Phase faults near the neutral were tested for different scenarios and are shown in Section V.B.

3) Stator Winding Turn Faults

Stator winding turn faults can occur in the slots or the end-winding region, depending on machine construction. To evaluate the sensitivity of turn faults for different levels of steady-state unbalances, the three branches were modeled with magnitude and phase unbalances (Section II.D). The standing split-phase current in secondary amperes is summarized in Table III. Fig. 11 shows the A-phase branch currents (ISP1A and ISP2A) along with the associated split-phase current (ISPA).

TABLE III
STANDING SPLIT-PHASE CURRENT APPLIED USING GENERATOR MODEL

Current	Offline	Online (Full Load)
IA	0.439 A sec	0.494 A sec
IB	0.000 A sec	0.006 A sec
IC	0.093 A sec	0.096 A sec
IN	4.31 A sec	4.67 A sec

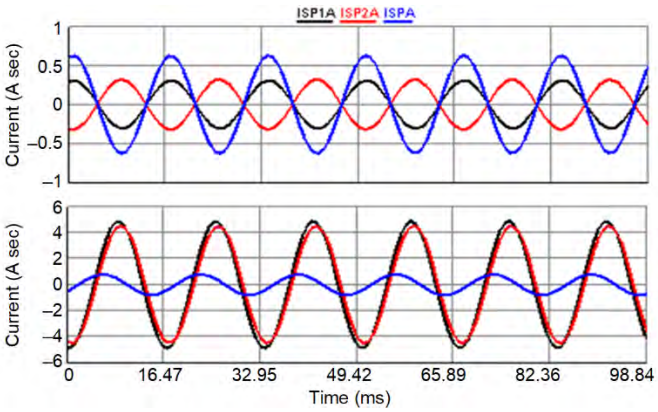

Fig. 11. Split-phase current for a generator model a) offline and b) online

Since the B-phase and C-phase unbalances were small, the interneutral CT measured the A-phase current and magnified it due to the lower CT ratio.

Seasonal variation can cause the split-phase current to be nearly twice as large on some generators [25], so the high-set elements (60PH/60NH) were set to twice the value. When the generator voltage is ramped, the split-phase current increases proportionately. Therefore, when the generator was offline, the low-set elements (60PL/60NL) were configured to reset and track the unbalance, which prevented them from operating.

4) *Series Faults*

Series faults were simulated on a single branch and on both branches. In instances where series faults are undetected, they can evolve to ground [27]. Fig. 12 shows series faults that evolved to ground on the terminal side (F2 and F4) and the neutral side (F3 and F5). These faults were simulated (see Section V.D) to verify the dependability of the different protection elements and provide application guidance.

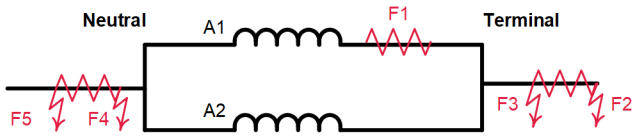

Fig. 12. Series fault locations tested

V. Results and Analysis

Protection security is an important consideration and was verified during testing. The validation testing confirmed the relay's ability to detect most internal faults. This section summarizes the sensitivity limits of the different protection elements for the internal faults discussed in Section IV.E.

A. *Intermittent Ground Faults*

Stator ground faults were applied throughout the winding at different load levels. This caused VG3 to vary from 3% to 8% of V_{NOMLG}. Ground faults near the generator terminal were protected by the 64G1 element. For ground faults near the generator neutral, the 64G2 element protected a higher percentage of the winding than the 64G3 element, especially for high levels of VG3. However, unlike the 64G3 element, the 64G2 element requires a third-harmonic survey [23] [28].

During the survey, it was noticed that the ratio of VN3 to VG3 (or VT3) was smaller at very low levels of the third harmonic (no load) compared to higher levels of the third harmonic (full load). This could be due to the fixed losses of the neutral grounding transformer (such as magnetizing current), which are supplied by the third-harmonic voltages. In contrast, the terminal VT losses are derived from the fundamental voltages and have less impact on the third-harmonic measurements. A similar observation has been made from field data [29].

1) *Terminal-Side Intermittent Stator Ground Fault*

Relevant relay measurements for a terminal-side ground fault with an arcing rate of 25% are shown in Fig. 13. When the A-phase voltage (VAZ in red) decreases, the neutral voltage (VBV in black) increases by the same amount. The 64G1 element asserts intermittently due to the arcing behavior of the fault. The 64G2 and 64G3 elements may also assert spuriously due to the transient third-harmonic filter response every time there is a step change in the voltages, due to the intermittent arcing nature of the fault.

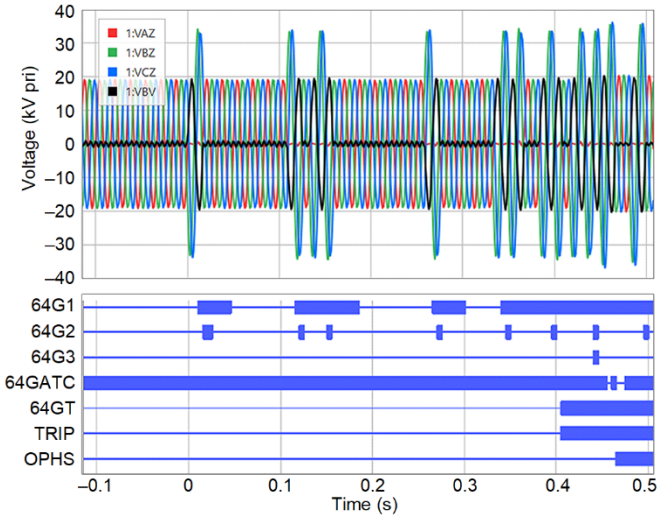

Fig. 13. Intermittent stator ground fault near the generator terminals

After a fault arcs a few times, the relay trips (64GT). Even after the breaker opens (OPHS indicates a terminal open phase), the fault continues to arc, and the voltages rise slightly, because the generator was running at full load prior to the trip.

In the past, generator relays would have delayed tripping for this type of fault. Modern generator relays can trip quicker for this condition due to the use of special timers and acceleration schemes noted in Section III.A.

2) *Neutral-Side Intermittent Stator Ground Fault*

Relevant relay measurements for a neutral-side ground fault with an arcing rate of 25% are shown in Fig. 14. The generator was at full load and producing 8% VG3. Both the 64G2 and 64G3 elements can detect and trip for this condition. The 64G2 element picks up more frequently, allowing for a quicker trip. Once the generator trips, the level of the third harmonic may be reduced, but the relay continues to detect the arcing ground fault.

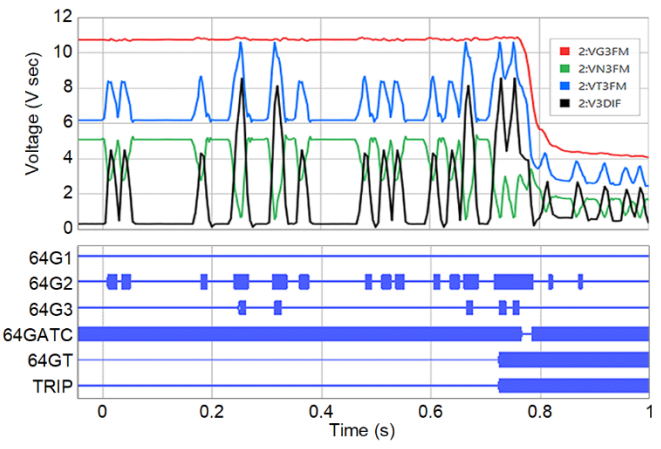

Fig. 14. Intermittent stator ground fault near the generator neutral

B. Phase Fault Sensitivity

1) Neutral-Side Faults

The 87G element is sensitive to all phase faults, even the most challenging ones located near the generator neutral. An internal fault at 1% of B1 and 1% of the C2 branch is shown in Fig. 15. The B-phase operate current (IOPB1) and restraint current (IRTB1) are shown; the C-phase currents are similar. The following observations can be made from Fig. 15:

- When the generator is online at full load, during the fault IOPB1 is 2.5 pu and IRTB1 is 4 pu. For 87G, the sensitive pickup and slope need to be set less than 2.5 pu and 60% to reliably trip for this fault.
- When the generator breaker is tripped (or at no load), the terminal side currents are zero. However, the generator continues to feed the fault from the neutral side, resulting in IOPB1 and IRTB1 equal to 2.5 pu.

To detect neutral-side faults, the 87G element (unlike an 87T element) utilizes the larger neutral-side currents to provide sensitive stator winding phase-fault protection. 87G sensitivity is not impacted by system strength since the system contribution to a neutral-side fault is negligible. The time-delayed split-phase elements would also trip for this fault.

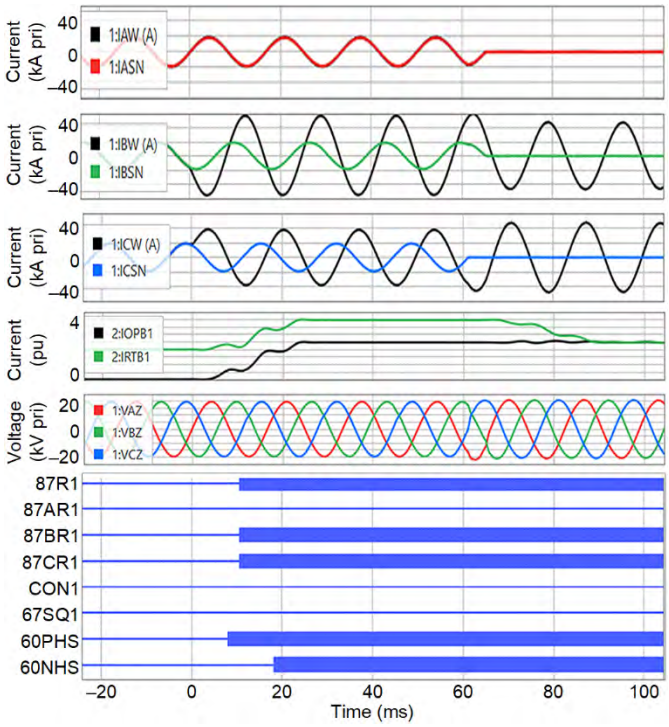

Fig. 15. Phase-to-phase fault near the generator neutral (1%)

2) Internal Fault During a Black-Start Scenario

Generators with black-start capability often need to energize a transformer that is external to the 87G zone. A black-start scenario was simulated by closing the low-voltage breaker shown in Fig. 16. An internal fault at 5% of the B1 and C2 branches developed 200 ms after the transformer was energized. The relay was in secure mode (CON1) with the default slope of 75%. It rode through the C-phase CT saturation when the fault occurred, and it marginally tripped. If coverage down to 1% is required for this application, which has an operate current of 2.25 pu and a restraint current of 3.70 pu, the secure slope would have to be set lower than 60%. A lower setting can be achieved by applying better CTs; a lower setting adds sensitivity for internal faults that evolve from external system conditions [24]. The 60P/60N elements also provide time-delayed coverage down to 1% of the winding.

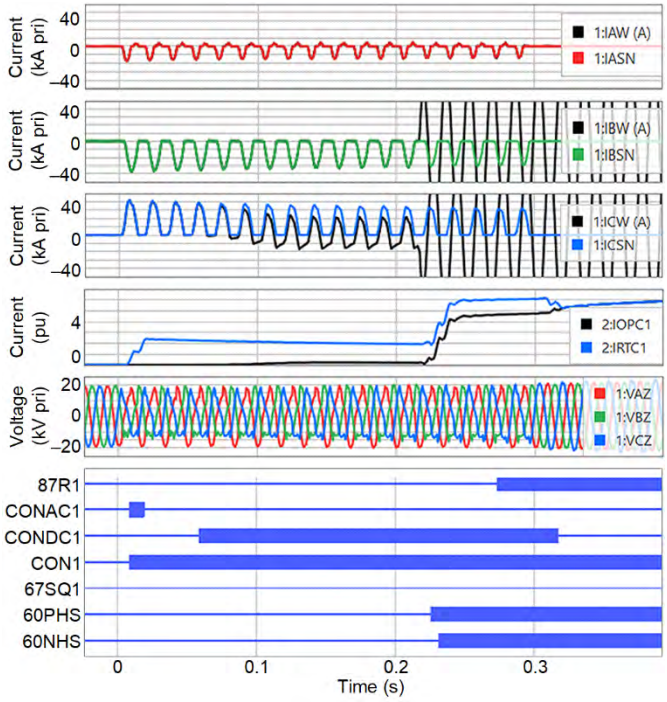

Fig. 16. Phase-to-phase fault near the neutral (5%) during a black start

C. Turn-to-Turn Fault Sensitivity

A survey of the stator winding diagram can help determine the possible turn fault locations for a particular machine [7]. The coverage provided by the different protection elements for a turn fault on one branch are summarized in Table IV. The minimum and the maximum percentages of turns that could be shorted in the model were 1% and 98%, respectively; the results in Table IV are extrapolated to 100%.

TABLE IV
GENERATOR PROTECTION ELEMENT COVERAGE FOR TURN-TO-TURN FAULTS

Element	Turns Shorted	Notes
67Q	10% to 100%	Online only
60PH	7% to 100%	Depends on faulted branch
60NH	7% to 100%	Depends on faulted branch
60PL	2% to 25%	Online only
60NL	2% to 25%	Online only

Fig. 17 shows a few of the relevant relay quantities for a turn fault that shorts 98% of the A1 branch.

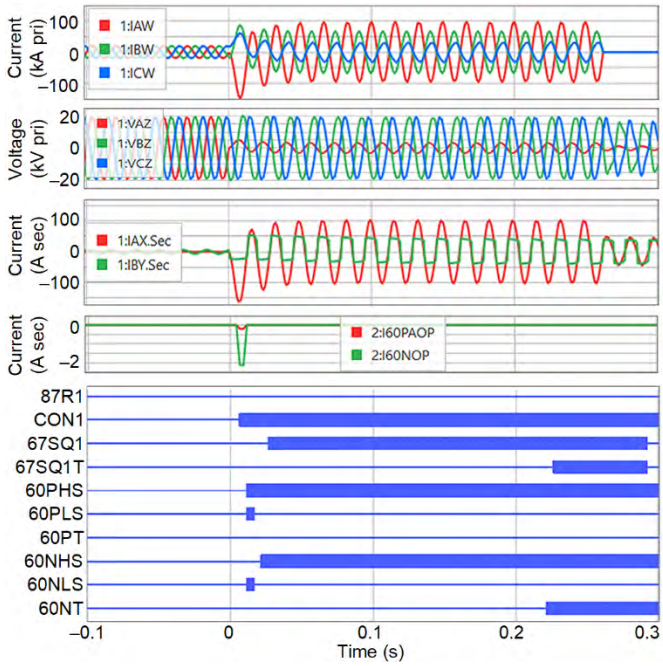

Fig. 17. Stator winding turn-to-turn fault shorting 98% of an A-phase branch

The 67Q, 60P, and 60N elements all operated for this fault, while 87G did not. The fault currents were severe enough that they appeared as an external event (CON1) to the 87G element, which prevented the sensitive 60PL and 60NL elements from operating. This is not an issue, because the other elements provide an overlap in coverage when a higher percentage of the winding is shorted.

Fig. 18 shows a few of the relevant relay quantities for a turn fault that shorts 2% of the A1 branch.

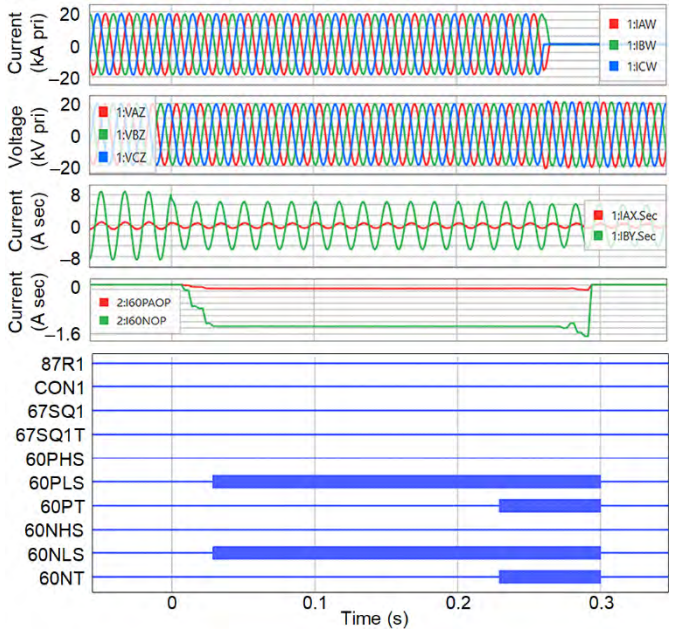

Fig. 18. Stator winding turn-to-turn fault shorting 2% of an A-phase branch

The phase currents and terminal voltages did not change much during the fault. Additionally, the circulating split-phase current went down since the fault was on the A1 branch and not the A2 branch. However, the adaptive, low-set 60PL and 60NL elements detected this fault, because they detected a change in the split-phase current.

1) 60P Sensitivity and Setting Considerations

The sensitivity of the 60P element is dependent on the winding configuration. The simplified circuit of Fig. 19 to evaluate split-phase currents is presented in [30], which also explains that to set the 60P pickup, the (3), (4), and (5) circuit equations may be applied.

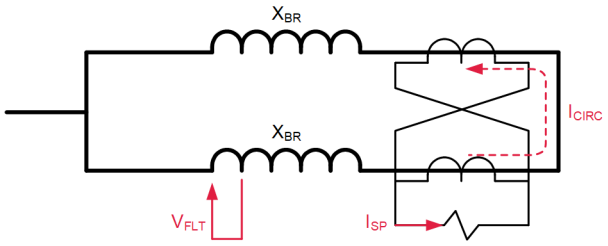

Fig. 19. Simplified circuit used to determine split-phase element pickup

$$X_{BR} = N_{BR} \bullet X_L \tag{3}$$

$$I_{CIRC} = \frac{V_{FLT}}{X_{BR} \bullet \left(1 - m + \frac{1}{N_{BR} - 1}\right)} \tag{4}$$

$$I_{SP} = \frac{2}{CTR_{SP}} \bullet I_{CIRC} \tag{5}$$

where:

m is the per-unit branch shorted.

X_{BR} is the leakage inductance of one branch.

N_{BR} is the number of branches per phase, two in this case.

I_{CIRC} is the circulating current from one branch to another.

I_{SP} is the split-phase current measured by the relay.

A comparison of the equations with the generator model simulations is shown in Fig. 20. For turn faults that short a small percentage of the winding, the simplified method overestimates the current by a factor of two.

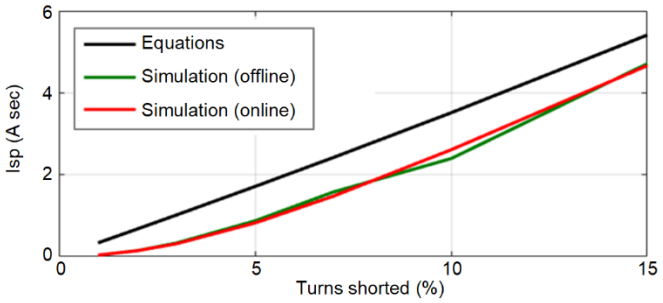

Fig. 20. Comparison of simplified split-phase equations with model response

This highlights the importance of leaving adequate margins or using simulation tools. Although the split-phase current magnitude seen by the protection is small, the unmeasurable fault current in the shorted turns for these low-percentage faults is large.

Fault current levels for turn faults are shown in Fig. 21, where the model reported the fault current in the generator when it was online and offline at nominal voltage. The values are similar to laboratory test data from a model generator [7].

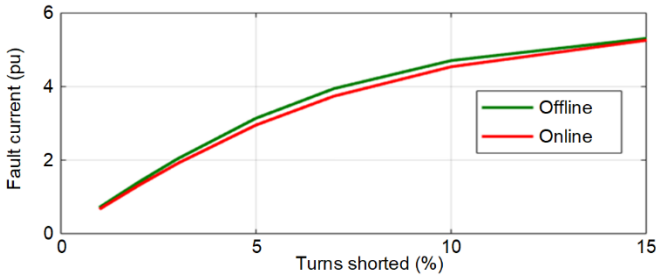

Fig. 21. Fault current levels for turn-to-turn faults

2) 67Q Sensitivity and Setting Considerations

The potential effectiveness of 67Q was evaluated during this validation. The sensitivity of the 67Q element is dependent on system strength. The equivalent negative-sequence circuit for a turn fault may be represented by Fig. 22. When the system is weak (i.e., large X_{SYS}) or the generator is offline, there is not enough I_2 for 67Q to detect the turn fault.

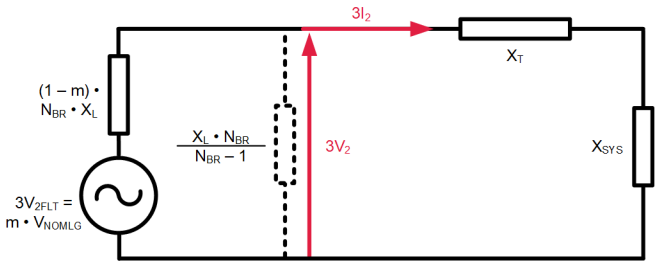

Fig. 22. Equivalent negative-sequence circuit to determine 67Q settings

To set the $3I_2$ pickup associated with the turn fault, (6)–(10) corresponding to the circuit of Fig. 22 can be applied. A comparison of the equations with simulated relay event records is shown in Fig. 23. The accuracy is typically within 20% and may be considered reasonable considering the ease of application.

$$X_{REV} = X_T + X_{SYS} \tag{6}$$

$$X_{EQ} = X_{REV} \,//\, \left(\frac{N_{BR}}{N_{BR}-1}\right) \bullet X_L \tag{7}$$

$$3V_{2FLT} = m \bullet V_{NOMLG} \tag{8}$$

$$3V_2 = 3V_{2FLT} \bullet \frac{X_{EQ}}{X_{EQ} + (1-m) \bullet N_{BR} \bullet X_L} \tag{9}$$

$$3I_2 = \frac{3V_2}{X_{REV}} \tag{10}$$

where:

X_{REV} is the system-side impedance measured from the generator terminals.

X_{EQ} is the equivalent impedance considering parallel branches. It is equal to X_{REV} for units with one branch per phase.

$3V_{2FLT}$ is the source associated with the turn fault.

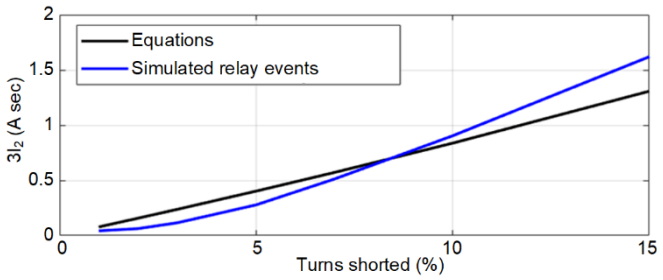

Fig. 23. Comparison of negative-sequence circuit equations with simulations

During full-load operation, the directional element described in (2) supervising 67Q is restrained by the positive-sequence current, which ensures that the ratio $a2 = I_2 / I_1$ is large enough (default of 0.10) to provide security for CT saturation or unbalance due to line asymmetries for a balanced three-phase fault. Because 67Q is applied at the generator terminals with the transformer impedance behind it, the unbalance associated with line asymmetry is not likely to be a significant factor, especially in strong systems. CT saturation is also not a concern, since the element can be applied with a fairly long time-delay, which drastically reduces CT requirements [24].

If additional sensitivity to detect turn faults from 67Q is required during full load, a2 may be reduced so that it does not prevent turn fault detection. For instance, with a 0.50 A pickup setting for the 67Q element that operates on $3I_2$ and generator nominal current of 3.34 A, a2 may be set to a value of $0.50 / (3 \bullet 3.34) = 0.05$. It is important to ensure that the generator unbalance current is normally well below this level.

D. Series Fault Sensitivity

The new model allows series faults to be simulated. These are challenging faults, and generator protection schemes typically do not cover them. When they occur, they are usually detected only after they have evolved to ground [27]. However, for the purpose of validating the new generator relay, series faults were applied near both the neutral side and terminal side of the stator winding (see Fig. 12).

1) Series Fault in a Single Branch

Series faults were applied on one branch of the model generator to evaluate protection performance on applications with multiple branches (for instance, most hydrogenerator units). The sensitivity of different generator protection elements that operated for a series fault during full load are summarized in Table V and can be referenced to a per-branch resistance and reactance of 6 mΩ and 208 mΩ, respectively.

TABLE V
MINIMUM SERIES FAULT RESISTANCE DETECTED BY PROTECTION ELEMENTS

Element	Fault Resistance	Notes
67Q	260 mΩ	Online only
60PH	70 mΩ	Depends on faulted branch
60NH	70 mΩ	Depends on faulted branch
60PL	10 mΩ	Online only
60NL	10 mΩ	Online only

Fig. 24 shows the relevant relay quantities for the 260 mΩ series fault. The 67Q element marginally operates, whereas the split-phase elements have enough operating current to detect the condition reliably.

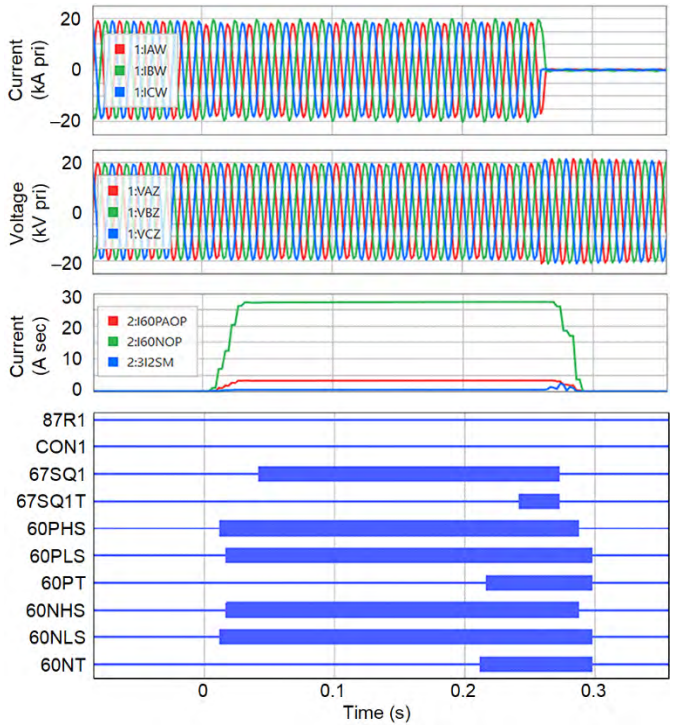

Fig. 24. Series fault on one branch with a resistance of 260 mΩ

2) Series Fault in One Phase Evolving to Ground

Series faults were applied on both branches of the A-phase to emulate the behavior of generators with one branch (for instance, most steam or gas turbine units). Because these conditions are not easily detected by generator protection, they typically evolve to ground before generator protection can operate.

a) Terminal-Side Series Fault Evolving to Ground

A terminal-side 75 mΩ series fault that evolved to ground near the A-phase terminals (F2 in Fig. 12) is shown in Fig. 25a and explained as follows.

The I_2 during this fault is due to the load current flowing through the fault resistance (R_F). This is unlike the single-branch series fault, where half the load current flows through R_F on one branch. Therefore, I_2 for a series fault is nearly four times as large (N_{BR}^2) for a fault on one phase compared to a fault on one branch. The 67Q element detects the series fault and can do so down to a fault resistance (R_F) of 60 mΩ. The authors recognize that these values represent a very large fault energy. The resistance of a series fault is still an open question, but field data from a series fault that evolved to ground suggest that these values are reasonable. Additionally, rapid tripping for a series fault stops damage to the generator in contrast to generator shunt faults (i.e., ground, phase, or turn faults).

During the series fault, the neutral voltage rises to 3.2 V. Due to the unbalance in the phase currents and the resulting elevated I_2, ground fault protection is not accelerated (64GATC = 0). The 64G1 element only detects the series fault if R_F is greater than 175 mΩ.

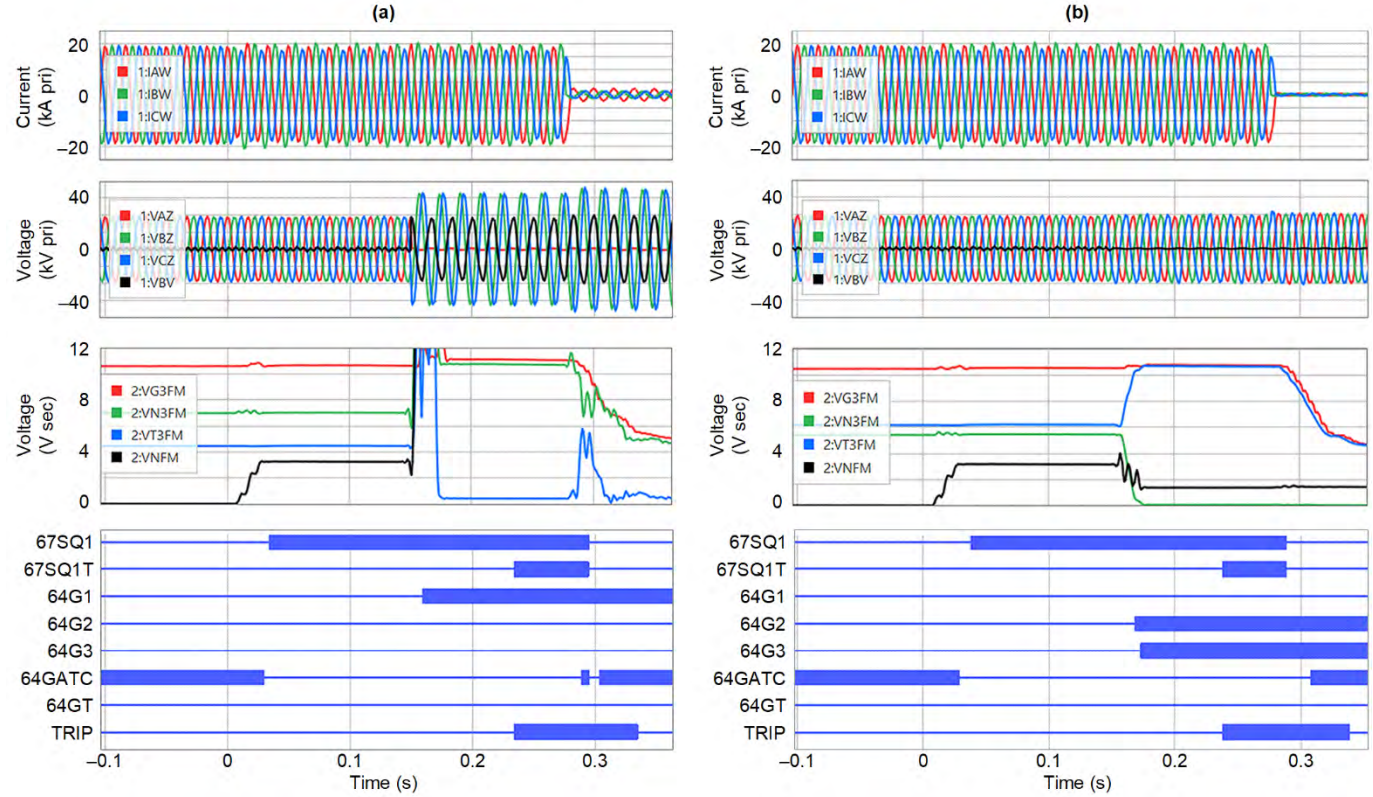

Fig. 25. Event reports for a) terminal-side and b) neutral-side series fault on A-phase evolving to ground

Once the fault evolves to ground (after 150 ms), 64G1 could trip for this condition. VN3 rises to VG3, and VT3 falls to zero, as expected from a terminal fault. If R_F and the resultant I_2 were small, the 64G1 trip would be accelerated. The authors recommend coordinating 67Q (e.g., 50Q pickup and a2 = 5% of I_{NOM}) and the 64G acceleration scheme (e.g., I_2 = 10% of I_{NOM}) so one of them can always trip quickly for this fault. A 5% V_2 used for 64G acceleration is adequate for higher R_F series faults, even in a weak system, and does not typically impact coordination.

b) Neutral-Side Series Fault Evolving to Ground

The same fault was then applied near the generator neutral and is shown in Fig. 25b. In this case, after the fault evolves to ground, VN3 goes to zero whereas VT3 equals VG3, allowing 64G2/64G3 to detect the fault reliably. VN goes down in this case since the ground was on the neutral side of the series fault (F5 in Fig. 12), but if it were on the terminal side (F4 in Fig. 12), it would go up slightly (e.g., to 9.5 V) and could aid tripping.

Nowadays, 67Q is not typically applied for generator protection, and third-harmonic schemes are often only configured to alarm. The event of Fig. 25b can be quite damaging and highlights the need to use protection elements such as 67Q and 64G2/64G3 to protect the generator.

VI. Conclusion

A faulted synchronous generator model has been developed for a real-time digital simulator and supports hardware-in-the-loop testing. This development allowed for the testing of protection element dependability for a new generator relay. Validation of the relay using the new model facilitated identification of application guidance that would otherwise have been difficult.

The stator ground fault protection elements, both neutral overvoltage and third-harmonic elements, were verified to operate quickly for intermittent faults near the generator terminal and neutral due to the use of acceleration schemes.

The generator differential was evaluated to be sensitive for all phase faults within the stator winding, as it can leverage the large neutral-side currents for faults near the neutral. For evolving external conditions (e.g., a black start) to an internal fault, the coverage may be reduced. Application considerations include employing better CTs or the use of time-delayed backup using split-phase protection.

The generator model supported the simulation of asymmetry between the stator parallel branches, which allowed comprehensive testing of split-phase protection elements, including those that track the associated standing split-phase current for added sensitivity. Use of the model also facilitated development and verification of new application guidance associated with the negative-sequence directional element. Similarly, existing guidance associated with split-phase protection was also evaluated.

Series faults were applied on one branch, which allowed for the comparison of sensitivity provided by the split-phase elements and the negative-sequence directional element.

Series faults on one phase that evolve to ground were applied. The negative-sequence directional element can detect the series fault if the level of unbalance is sufficient. Ground fault protection can detect the fault after ground is involved. This paper recommends coordinating the ground fault acceleration scheme and negative-sequence directional element settings to ensure reliable tripping for these damaging conditions.

VII. Appendix

A summary of relevant relay settings used for this paper is presented in Table VI–Table X.

A 67Q pickup of 0.50 A and a2 of 5% is set above any normal unbalance (Section V.C.2). For this paper, the I_2 pickup associated with 46Q11 in the 64GATC setting of Table VI was set to 6% based on machine capability using state-of-the-art knowledge. However, per guidance from Section V.D.2, it is preferable to use the same currents as 67Q (at the generator terminal), apply dedicated logic/level, and set the I_2 pickup greater than 10% of I_{NOM} to coordinate with 67Q. There will be plenty of I_2 for a system ground fault that may cause 64G1 to operate, so choosing a large value is not an issue [21].

The 3V2ZM < 10 V check should work for most applications that use a neutral grounding transformer for 64G1 and that use the terminal VTs to measure V_2.

Acceleration may not be provided (i.e., 64GATC = 0) for a CT failure or a loss-of-potential condition.

Table VI
Stator Ground Protection Element (64G) Settings

Setting	Value	Notes
64G1P1	6.9 V	Covers down to 5% of the winding [28]
64G2R1	0.87	Used survey and spreadsheet [28]
64G2P1	2.59 V	Used survey and spreadsheet [28]
64G3R1	0.15	Covers 15% of the winding [23]
64G3P1	1.40 V	VG3 = 1% • VNOMLG / PTRV2 [23]
64GATC	NOT 46Q11 AND 3V2ZM < 10	Explained in the appendix description; set to 3I2SM < 10% (1 A) and 3V2ZM < 5% (10 V) instead
64GAPU	0.200 s	Default accelerated 64G pickup delay

Table VII
Generator Differential Element (87G) Settings

Setting	Value	Notes
INOMGS	3.34 A	Generator secondary nominal current
87P11	0.25 pu	Default sensitive pickup
87P21	0.50 pu	Default secure pickup for black start [24]
87SLP1	10%	Default sensitive slope
87SLP2	75%	Default secure slope, depends on CTs [24]
87EFDO1	1.0 s	Default dropout, also used to reset 60PL/60NL

TABLE VIII
NEGATIVE-SEQUENCE DIRECTIONAL ELEMENT (67Q) SETTINGS

Setting	Value	Notes
50SQ1P	0.50 A	Forward $3I_2$ overcurrent threshold
67SQ1TC	SF32Q	Forward unbalanced fault detected
Z1ANGS	88.4°	Impedance angle of transformer plus system
50QPS	0.50 A	Directional element $3I_2$ pickup
Z2FS	–0.83 Ω	50% of transformer leakage (X_T)
Z2RS	+0.62 Ω	30% of stator leakage reactance (X_L)
A2S	0.05	I_2/I_1 > normal unbalance (Section V.C.2)

TABLE IX
SPLIT-PHASE PROTECTION ELEMENT (60P) SETTINGS

Setting	Value	Notes
60PAHP	1.00 A	High-set pickup A-phase (Section IV.E.3)
60PpHP	0.25 A	High-set pickup B-/C-phase (Section IV.E.3)
60PHD	1.0 s	Secure delay
60PpHSS	0	High-set security switch for all phases
60PpLP	0.10 A	Low-set pickup
60PLD	0.200 s	Low-set delay
60PLR	NOT 52A_S OR CON1	Low-set element reset; tracks the standing error during startup and disturbance
60PLT	1 s	Fast time constant for additional security
60PpLSS	0	Low-set security switch for all phases

TABLE X
NEUTRAL SPLIT-PHASE PROTECTION ELEMENT (60N) SETTINGS

Setting	Value	Notes
60NHP	10 A	High-set pickup (Section IV.E)
60NHD	1.0 s	Secure delay
60NHSS	0	High-set security switch
60NLP	1 A	Low-set pickup
60NLD	0.200 s	Low-set delay
60NLR	NOT 52_A OR CON1	Low-set element reset; tracks the standing error during startup and disturbance
60NLT	1 s	Fast time constant for additional security
60NLSS	0	Low-set security switch

VIII. REFERENCES

[1] D. Finney, M. Adamiak, and B. Kasztenny, "Dynamic Testing of Generator Protection Using a Model Generator Platform," proceedings of the 56th Annual Georgia Tech Protective Relaying Conference, Atlanta, GA, 2002.

[2] H. W. Dommel, "Digital Computer Solution of Electromagnetic Transients in Single-and Multiphase Networks," *IEEE Transactions on Power Apparatus and Systems*, Vol. PAS-88, Issue 4, April 1969, pp. 388–399.

[3] J. D. Gao, L. Z. Zhang, and X. H. Wang, "AC Machine Systems: Mathematical Model and Parameters, Analysis, and System Performance," Tsinghua University Press, Beijing, China, 2009.

[4] V. A. Kinitsky, "Inductances of a Portion of the Armature Winding of Synchronous Machines," *IEEE Transactions on Power Apparatus and Systems*, Vol. 84, Issue. 5, May 1965, pp. 389–396.

[5] N. A. Al-Nuaim and H. A. Toliyat, "A Novel Method for Modeling Dynamic Air-Gap Eccentricity in Synchronous Machines Based on Modified Winding Function Theory," *IEEE Transactions on Energy Conversion*, Vol. 13, Issue 2, June 1998, pp. 156–162.

[6] A. I. Megahed and O. P. Malik, "Simulation of Internal Faults in Synchronous Generators," *IEEE Transactions on Energy Conversion*, Vol. 14, Issue 4, December 1999, pp. 1306–1311.

[7] R. Chowdhury, D. Finney, and N. Fischer, "Using the Multi-Loop Fault Analysis Method for Setting and Evaluating Generator Protection Elements," proceedings of the 71st Annual Conference for Protective Relay Engineers, College Station, TX, March 2018.

[8] H. W. Dommel, "Digital Computer Solution of Electromagnetic Transients in Single- and Multiphase Networks," *IEEE Transactions on Power Apparatus and Systems*, Vol. PAS-88, Issue 4, April 1969, pp. 388–399.

[9] RTDS Technologies Inc., *RTDS User's Manual*, Winnipeg, Canada, 2019.

[10] A. B. Dehkordi, P. Neti, A. M. Gole, and T. L. Maguire, "Development and Validation of a Comprehensive Synchronous Machine Model for a Real-Time Environment," *IEEE Transactions on Energy Conversion*, Vol. 25, Issue 1, February 2010, pp. 34–48.

[11] A. B. Dehkordi, A. M., Gole, and T. L. Maguire, "Permanent Magnet Synchronous Machine Model for Real-Time Simulation," proceedings of the International Conference on Power Systems Transients 2005, Montreal, Canada, June 2005.

[12] C. V. Jones, *The Unified Theory of Electrical Machines*, Plenum Press, New York, NY, 1967.

[13] A. B. Dehkordi, "Improved Models of Electric Machines for Real-Time Digital Simulation," PhD thesis, University of Manitoba, 2010.

[14] A. Tessarolo, "Modeling and Analysis of Multiphase Electric Machines for High-Power Applications," PhD thesis, University of Trieste, 2011.

[15] X. Luo, Y. Liao, H. A. Toliyat, A. El-Antably, and T. A. Lipo, "Multiple Coupled Circuit Modeling of Induction Machines," *IEEE Transactions on Industry Applications*, Vol. 31, Issue 2, March 1995, pp. 311–318.

[16] N. A. Al-Nuaim and H. A. Toliyat, "A Novel Method for Modeling Dynamic Air-Gap Eccentricity in Synchronous Machines Based on Modified Winding Function Theory," *IEEE Transactions on Energy Conversion*, Vol. 13, Issue 2, June 1998, pp. 156–162.

[17] P. P. Reichmeider, C. A. Gross, D. Querrey, D. Novosel, and S. Salon, "Internal Faults in Synchronous Machines, Part I: The Machine Model," *IEEE Transactions on Energy Conversion*, Vol. 15, Issue 4, December 2000, pp. 376–379.

[18] P. P. Reichmeider, D. Querrey, C. A. Gross, D. Novosel, and S. Salon, "Internal Faults in Synchronous Machines, Part II: Model Performance," *IEEE Transactions on Energy Conversion*, Vol. 15, Issue 4, December 2000, pp. 380–385.

[19] P. S. Kundur, *Power System Stability and Control*, McGraw-Hill, New York, NY, 1983.

[20] *SEL-400G Advanced Generator Protection System Instruction Manual*. Available: selinc.com.

[21] IEEE Power and Energy Society, "Improved Generator Ground Fault Schemes," Technical Report PES-TR 82, September 2020.

[22] G. Koeppl and D. Braun, "New Aspects for Neutral Grounding of Generators Considering Intermittent Faults," proceedings of CIDEL (Congreso Internacional de Distribución Eléctrica) Argentina 2010, Buenos Aires, Argentina, September 2010.

[23] R. Chowdhury, D. Finney, N. Fischer, and J. Young, "Generator Third Harmonic Protection Explained," proceedings of the 71st Annual Conference for Protective Relay Engineers, College Station, TX, March 2018.

[24] R. Chowdhury, D. Finney, N. Fischer, and D. Taylor, "Determining CT Requirements for Generator and Transformer Protective Relays," proceedings of the 74th Annual Conference for Protective Relay Engineers, virtual format, March 2021.

[25] S. Kim, D. Finney, N. Fischer, and B. Kasztenny, "CT Requirements for Generator Split-Phase Protection," proceedings of the 38th Annual Western Protective Relay Conference, Spokane, WA, October 2011.

[26] J. DeHaan, "Electrical Unbalance Assessment of a Hydroelectric Generator With Bypassed Stator Coils," proceedings of the IEEE International Electric Machines and Drives Conference, Seattle, WA, May 1999.

[27] C. V. Maughan, "Incapability of Analog Relay Protection to Detect Generator Stator Winding Ground Failures at Neutral End," proceedings of the 2013 IEEE Electrical Insulation Conference, Ottawa, ON, Canada, June 2013.

[28] L. Underwood, J. Young, and D. Finney, "Setting the 64G1 and 64G2 Elements in SEL Generator Protection Relays," SEL Application Guide (AG2005-08), 2020. Available: selinc.com.

[29] R. Chowdhury, M. Rusicior, J. Vico, and J. Young, "How Transformer DC Winding Resistance Testing Can Cause Generator Relays to Operate," proceedings of the 69th Annual Conference for Protective Relay Engineers, College Station, TX, April 2016.

[30] D. Finney, B. Kasztenny, M. McClure, G. Brunello, and A. LaCroix, "Self-Adaptive Generator Protection Methods," proceedings of the 60th Annual Georgia Tech Protective Relaying Conference, Atlanta, GA, May 2006.

IX. Biographies

Ali B. Dehkordi received BSc and MSc degrees in electrical engineering from Sharif University of Technology, Tehran, Iran, and a PhD degree from the University of Manitoba, Canada, in 1999, 2002, and 2010, respectively. Between 1998 and 2002, he worked on various industrial projects that included substation and transformer maintenance as well as power quality projects. His research interests are on the modeling of power system and power electronic components, in particular electric machines for Electromagnetic Transient Programs and Real Time Digital Simulation, the area that he has been working on for over 18 years. Dr. Dehkordi is a recipient of Dennis Woodford Prize for "the most outstanding graduate thesis dealing with power system modeling and simulation." He is currently employed by RTDS Technologies Inc., located in Winnipeg, Canada. He is a senior member of IEEE.

Ritwik Chowdhury received his BS degree in engineering from the University of British Columbia, and his MS degree in engineering from the University of Toronto. He joined Schweitzer Engineering Laboratories, Inc. (SEL) in 2012, where he has worked as an application engineer and is presently a senior engineer in the research and development division. Ritwik holds 5 patents and has authored 20 technical papers in the area of power system protection and point-on-wave controlled switching. He is a member of the IEEE PSRC main committee and the chairman of two IEEE Standards Working Groups. He is a senior member of the IEEE and a registered professional engineer in the province of Ontario.

Normann Fischer received a Higher Diploma in Technology, with honors, from Technikon Witwatersrand, Johannesburg, South Africa, in 1988; a BSEE, with honors, from the University of Cape Town, in 1993; an MSEE from the University of Idaho in 2005; and a PhD from the University of Idaho in 2014. He joined Eskom as a protection technician in 1984 and was a senior design engineer in the Eskom protection design department for three years. He then joined IST Energy as a senior design engineer in 1996. In 1999, Normann joined Schweitzer Engineering Laboratories, Inc. (SEL), where he is currently a distinguished engineer in research and development. He was a registered professional engineer in South Africa and a member of the South African Institute of Electrical Engineers. He is currently a senior member of IEEE and a member of the American Society for Engineering Education (ASEE). Normann has authored over 60 technical and 10 transaction papers and holds over 20 patents related to electrical engineering and power system protection.

Dale Finney received his bachelor of engineering degree from Lakehead University, and his master of engineering degree from the University of Toronto. He began his career with Ontario Hydro, where he worked as a protection and control engineer. Currently, he is employed as a principal power engineer with Schweitzer Engineering Laboratories, Inc. (SEL). He holds more than 10 patents and has authored more than 30 papers in the area of power system protection. He is a member of the main committee and past chair of the rotating machinery subcommittee of the IEEE PSRC committee. He is a senior member of the IEEE and a registered professional engineer in the province of Nova Scotia.